

## Quasiharmonic lattice-dynamics and molecular-dynamics calculations for the Lennard-Jones solids

Raffaele Guido Della Valle and Elisabetta Venuti

*Dipartimento di Chimica Fisica e Inorganica, Università di Bologna, Viale Risorgimento 4, I-40136 Bologna, Italy*

(Received 16 October 1997)

We present molecular-dynamics (MD), quasiharmonic lattice-dynamics (QHLD), and energy-minimization calculations for the crystal structure of Ne, Ar, Kr, and Xe as a function of pressure and temperature. Lennard-Jones parameters are obtained for Ne, Kr, and Xe to reproduce the experimental pressure dependence of the density. We employ a simple method that combines results of QHLD and MD calculations to achieve densities in good agreement with experiment from 0 K to melting. Melting is discussed in connection with intrinsic instability of the solid as given by the QHLD approximation. [S0163-1829(98)02825-2]

### I. INTRODUCTION

Lattice dynamics (LD) is based on the expansion of the potential energy of the crystal in powers of the displacements of the atoms from a reference structure.<sup>1,2</sup> The harmonic approximation, in which the expansion is truncated at the second order, reduces the many-body problem to many exactly soluble one-body problems and allows a direct computation of all thermodynamic functions. Harmonic<sup>1</sup> and quasiharmonic<sup>3-5</sup> lattice dynamics (HLD and QHLD) are alternative LD strategies, which differ in the choice of the reference structure. For HLD this is the minimum potential energy (mechanical equilibrium) structure, whereas for QHLD it is the minimum free energy (thermodynamic equilibrium) average structure at a given temperature  $T$  and pressure  $p$ . This difference is crucial, because the accuracy of the harmonic approximation is controlled by the amplitude of the displacements from the reference structure. Therefore QHLD might remain accurate in regimes where the average structure deviates significantly from that of the potential minimum, provided that the amplitude of the vibrations around the average does not grow too large. Conventional HLD is definitely unusable in these situations.

A straightforward way to assess the accuracy of the QHLD approximation is to choose a model system and to compare the QHLD calculations with the essentially "exact" classical mechanics results of molecular-dynamics (MD) or Monte Carlo (MC) simulations.<sup>6</sup> If the same model system and interaction potential are employed for both QHLD and the classical simulations, all differences between the two sets of results must be due to the approximations implicit in the two methods.

Lacks and Rutledge<sup>7</sup> have chosen a monoatomic fcc lattice with Lennard-Jones (LJ) interactions as a model to study the behavior of the QHLD and MC free energies as a function of  $T$ . They find that the QHLD free energy is reasonably accurate up to  $T_m/2$ , and rapidly deteriorates above that; here  $T_m$  is the melting temperature. These results clearly indicate that QHLD as such is not reliable close to  $T_m$ . However, since not all observables behave in the same way,<sup>7</sup> a general statement is not yet possible. In fact it is conceivable, though unlikely, that specific quantities might deteriorate so slowly

with increasing  $T$  as to remain usable up to  $T_m$ . There are *a posteriori* hints that this behavior might hold for the crystallographic parameters. In fact, in recent QHLD calculations for naphthalene,<sup>8</sup> benzene,<sup>9</sup> and argon<sup>10</sup> we obtained structural results in acceptable agreement with the experiments in the whole range of existence of the solids. Since close to  $T_m$  the amplitude of the atomic vibrations are large and the harmonic approximation is not expected to be accurate, these results require further investigation. To check whether the good results for the crystallographic structure near  $T_m$  were a genuine consequence of the method, we have performed QHLD and MD calculations for the structures of the Ne, Ar, Kr, and Xe crystals as a function of  $p$  and  $T$ .

Following Lacks and Rutledge,<sup>7</sup> we started this project<sup>10</sup> by using Verlet's<sup>11</sup> LJ parameters for argon. These parameters are known to give good agreement with the experimental properties of solid, liquid, and gaseous argon if many-body interactions are neglected.<sup>11,12</sup> With this effective two-body potential we obtained<sup>10</sup> excellent QHLD results for the density  $\rho$ , at least for very low  $T$ .

Given the excellent results for Ar, we expected similarly good behavior for the heavier rare gases, Kr and Xe. We tried more than 20 different LJ models from standard compilations<sup>6,13-17</sup> and, much to our amazement, none of them gave sensible results. All QHLD calculations with these models gave large discrepancies with the experimental densities at low  $T$ : these are precisely the conditions where QHLD was supposed to be accurate. Even more puzzling was the fact that the *experimental* density did not follow any regular trend with the atomic number once reduced with the literature LJ parameters. Since the experimental data for Ne, Ar, Kr, and Xe do follow a regular trend when reduced with respect to the critical point data ( $\rho_c$ ,  $T_m$ ,  $p_c$ ),<sup>13</sup> we have concluded that the origin of the discrepancies is the usage of inappropriate LJ parameters.

Perhaps one could have forecast these kinds of difficulties, since most of the literature parameters<sup>6,13-17</sup> are fitted to data on the gas, rather than the solid. The gas data yield, in principle, the true interaction potential between two isolated atoms, whereas for the solid and liquid phases one needs effective two-body models. Such LJ models incorporate an average of the many-body interactions and, therefore, can

only be valid in a limited density range. We wish to stress that we do not believe that the true interaction potential in the rare gases follow a LJ curve, nor that the literature parameters are “wrong.” We aim to map the experimental behavior of the rare-gas solids onto properly chosen LJ models. Since there are two adjustable potential parameters, it is always possible to obtain exact agreement between experiments and calculations for at least two  $p, T$  points, and approximate agreement for a limited range of  $p, T$  values. For our purposes we require agreement at low  $p$  and  $T$  (the regime where QHLD is accurate), and we have therefore decided to adjust the LJ models to low  $p, T$  data. Different choices may be appropriate for other purposes.

## II. METHODS

### A. Molecular dynamics

MD (Ref. 6) is a simulation method in which the classical mechanical equations of motion of the system are integrated numerically. The method avoids any assumption of harmonicity of the lattice vibrations, at the cost of neglecting all quantum effects. We use the MD results as calibration data to investigate the convergence of the QHLD results towards the classical limit, and to evaluate the effects of the vibrational anharmonicity.

We performed a sequence of MD simulation runs for a specified number of particles  $N$ , pressure  $p$ , and temperature  $T$ . The simulations employed  $N=256$  particles, in a cube with periodic boundary conditions, and, using Andersen’s isothermal-isobaric method,<sup>18</sup> described an fcc crystal in contact with a heat bath and subject to a hydrostatic pressure. The equations of motion were integrated using the velocity Verlet algorithm.<sup>11,19</sup> Since numerous MD studies of monoatomic LJ systems have been reported,<sup>6,11,19</sup> we omit other details of the present simulation.

### B. Quasiharmonic lattice dynamics

In the QHLD method<sup>3-5</sup> the Gibbs free energy of the crystal is computed as the free energy of an ensemble of phonons of frequency  $\nu_i$ :

$$G(p, T) = \Phi_0 + pV + \sum_i \frac{h\nu_i}{2} + k_B T \sum_i \ln \left[ 1 - \exp\left(-\frac{h\nu_i}{k_B T}\right) \right]. \quad (1)$$

Here  $\Phi_0$  is the total potential energy of the crystal in its average structure (the electronic ground-state energy),  $pV$  is the pressure-volume term,  $\sum h\nu_i/2$  is the zero-point energy, and the last term is the entropic contribution. The structure as a function of  $p$  and  $T$  is determined by minimizing  $G$  with respect to the unit-cell volume. Further details of the QHLD method appear in Refs. 8–10.

For comparison with the MD calculations, where quantum effects are neglected, it is appropriate to consider the classical limit (i.e.,  $h \rightarrow 0$ ) of Eq. (1):<sup>4</sup>

$$G_{\text{classical}}(p, T) = \Phi_0 + pV + k_B T \sum_i \ln \left( \frac{h\nu_i}{k_B T} \right). \quad (2)$$

It should be noticed that, although Eq. (2) still depends on Planck’s constant  $h$ , its derivatives, and thus the equilibrium

TABLE I. Data for the rare gases. The table lists LJ potential parameters  $\epsilon$  and  $\sigma$ , mass  $m$ , reduced Planck constant  $h^* = h/\sqrt{m\sigma^2\epsilon}$ , and experimental<sup>15</sup> and computed melting temperatures  $T_m^{\text{exp}}$  and  $T_m$ . LJ parameters for Ar are from Ref. 11; those for Ne, Kr, and Xe are from our fits.

	$\epsilon$ (K)	$\sigma$ (Å)	$m$ (amu)	$h^*$	$T_m^{\text{exp}}$ (K)	$T_m$ (K)
Ne	38.5	2.786	20.183	0.563	24.553	22
Ar	119.8	3.405	39.948	0.186	83.806	78
Kr	159.9	3.639	83.8	0.104	115.763	105
Xe	220.9	3.962	131.3	0.065	161.391	145

crystal structure, do not. The difference between  $G_{\text{classical}}$  and  $G$  equals the zero point energy at 0 K, and, as appropriate for a classical limit, tends to disappear at very high  $T$  ( $k_B T \gg h\nu_i$ ).

If all vibrational effects are neglected (the static lattice approximation), both  $G$  and  $G_{\text{classical}}$  reduce to the purely mechanical part of the Gibbs free energy,  $G_{\text{mech}}(p) = \Phi_0 + pV$ , which is the free energy in the limit of a large atomic mass. An energy minimization (EM) calculation for  $G_{\text{mech}}$  avoids the determination of the phonon frequencies and is therefore less time consuming than the complete calculation.

## III. CALCULATIONS

We have used MD and QHLD to compute, as a function of  $p$  and  $T$ , the structure of a monoatomic fcc lattice with pairwise additive LJ interactions,  $\Phi(r) = 4\epsilon[(\sigma/r)^{12} - (\sigma/r)^6]$ . To compare different atomic species we use non-dimensional reduced units, e.g., temperature  $T^* = T/\epsilon$ , pressure  $p^* = p\sigma^3/\epsilon$ , and density  $\rho^* = \rho\sigma^3/m$ ; here  $m$  is the atomic mass. This is the standard approach in LJ calculations for monoatomic systems.<sup>6,11,19</sup> When expressed in reduced units, the MD,  $G_{\text{classical}}$ , and  $G_{\text{mech}}$  results turn out to be independent of the atomic species, because the classical mechanics system has no energy, length and mass scales other than  $\epsilon$ ,  $\sigma$ , and  $m$ . On the other hand, the experiments and the QHLD results with the quantum free energy  $G$  [Eq. (1)] depend on Planck’s constant  $h$ , which in reduced units reads  $h^* = h/\sqrt{m\sigma^2\epsilon}$ , and are therefore dependent on the atomic number  $Z$ .<sup>20</sup> Because  $h^*$  tends to zero for large  $Z$  (as  $m$ ,  $\sigma$ , and  $\epsilon$  all increase with  $Z$ ), the reduced data should monotonically converge towards a classical limit in the sequence Ne, Ar, Xe, Kr.

## IV. RESULTS

### A. Argon density as a function of pressure

In the calculations for solid Ar we have used Verlet’s<sup>11</sup> LJ parameters (Table I). We report in Fig. 1 the results for the argon density  $\rho$  as a function of pressure  $p$ . The measured  $\rho$  vs  $p$  at 4, 77, and 293 K (Refs. 21 and 22) are compared to the corresponding MD and QHLD results. The main body of the figure contains the data for moderate pressures,  $p \leq 2$  GPa, which we discuss first. At 4 K, where the anharmonicity is negligible, QHLD reproduces the low  $p$  measurements almost perfectly, while MD, which neglects the

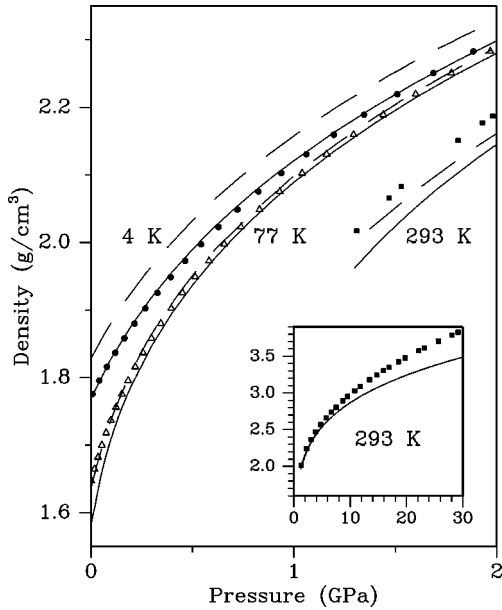


FIG. 1. Argon density  $\rho$  (g/cm<sup>3</sup>) vs pressure  $p$  (GPa). Symbols: experiments (Refs. 21 and 22) at 4 K (circles), 77 K (triangles), and 293 K (squares). Curves: calculations with MD (broken lines) and QHLD (solid lines). The data at 293 K are also reproduced in the inset, for pressures up to 30 GPa (Ref. 22). The MD and QHLD curves are not distinguishable at the scale of the inset.

zero-point expansion on the lattice, overestimates the experimental density. At higher  $T$ , where anharmonicity is large but quantum effects are less important, the opposite situation holds and MD is found to be more accurate than QHLD. The difference between MD and QHLD is only noticeable at very low  $p$  and tend to vanish for increasing  $p$ .

The good results of the LJ model for  $p \leq 2$  GPa do not extend to higher pressures, as shown by the inset of Fig. 1 for the results up to 30 GPa. Since in this  $p$  range MD and QHLD are barely distinguishable and both disagree with the experiments,<sup>22</sup> the failure of the calculations must be due to deficiencies of the potential, rather than to the calculation method. After analyzing their high  $p$  data, Grimsditch, Loubeyre, and Polian<sup>22</sup> have stated that for very dense solid argon there is no way to reproduce the experimental results with a pair potential and that many-body potentials have to be incorporated. Even though it is not yet ruled out that an effective pair potential with a different functional form could work, it is clear that the Verlet's LJ model<sup>11</sup> is not usable beyond 2 GPa.

### B. Dependence of the density on the atomic species

As discussed in the Introduction, none of the literature LJ models for Ne, Kr, and Xe that we have tested<sup>6,13-17</sup> was found appropriate for our purposes. We have therefore developed new LJ models by fitting the QHLD calculations to the density measurements as a function of  $p$  at the lowest available  $T$  and in a range of moderate pressures (0–2 GPa). This is the regime where the harmonic approximation is valid and, as shown by the results for Ar, effective two-body LJ models are usable. The optimal LJ parameters, which are reported in Table I, have values in the ranges of the typical literature models. The Ne, Kr, and Xe data<sup>21,23</sup> used in the fit

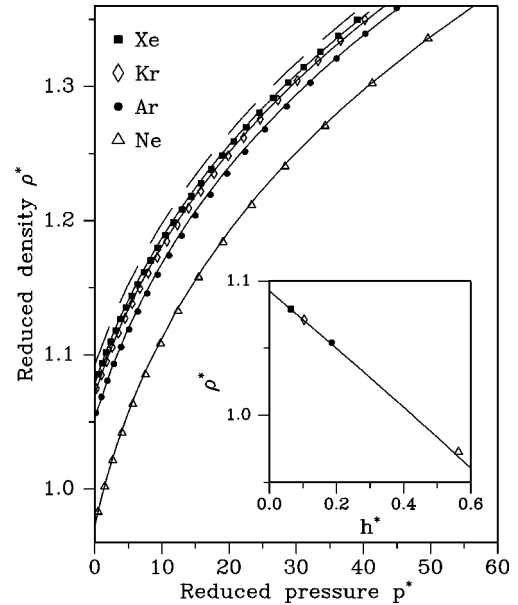


FIG. 2. Reduced density  $\rho^* = \rho\sigma^3/m$  vs reduced pressure  $p^* = p\sigma^3/\epsilon$  for the rare gases at low temperatures ( $T \approx 0$ ). Experiments at 4 K for Ne (Ref. 23), Ar, Kr, and Xe (Ref. 21): symbols as indicated in the figure. QHLD calculations with  $G$  and  $G_{\text{mech}}$ : solid and broken lines, respectively. The inset displays  $\rho^*$  vs  $h^* = h/\sqrt{m\sigma^2\epsilon}$  at  $p=0$ : QHLD calculations at  $T=0$  (solid line) and experiments (Ref. 32) on Ne at 3 K, Ar, and Kr at 4 K, and Xe at 5 K (symbols).

are compared in Fig. 2 with the QHLD results with the optimal LJ models. The Ar measurements and calculations at 4 K already shown in Fig. 1 are also reproduced in Fig. 2, together with the results of an EM calculation for  $G_{\text{mech}}$  (static lattice approximation), which in reduced units is independent of the atomic species.

The good agreement between experiments and calculations in Fig. 2 has no particular significance, as it merely indicates that the fits are good. Of greater importance is the fact that the experimental data, when reduced with this particular set of  $\epsilon$  and  $\rho$  values, follow a sensible trend with the atomic mass  $m$ . The reduced density  $\rho^*$  is lower for Ne, which has the lighter atom and therefore the largest zero-point effects, and then increases with  $m$ . As the classical limit is approached in the Ne, Ar, Kr, Xe sequence, the experimental  $\rho^*$  tends to a limiting curve, which appears to be very close to the static lattice calculations for infinite  $m$ . The  $G_{\text{mech}}$  results, which can be obtained very economically, can be a useful approximation if one wants to estimate the effects of pressure without all the complications of a complete QHLD calculation.

To clarify the role of the quantum effects on the density, we have computed  $\rho^*(p, T)$  at zero  $p$  and  $T$  as a function of  $m$ , considered as a continuously varying parameter. The resulting  $\rho^*$  is displayed as a function of  $h^* = h/\sqrt{m\sigma^2\epsilon}$  in the inset of Fig. 2, together with the experimental data at the lowest available  $T$  and  $p$ . These data constitute, in effect, a vertical cross section of Fig. 2 along the  $p=0$  line. Since the  $\rho^*(0,0)$  vs  $h^*$  curve does not depend on any physical dimension, all the experimental data at  $p \approx 0, T \approx 0$ , if properly reduced, should lie close to the curve. This is what happens with the LJ parameters of Table I, but not with the other LJ

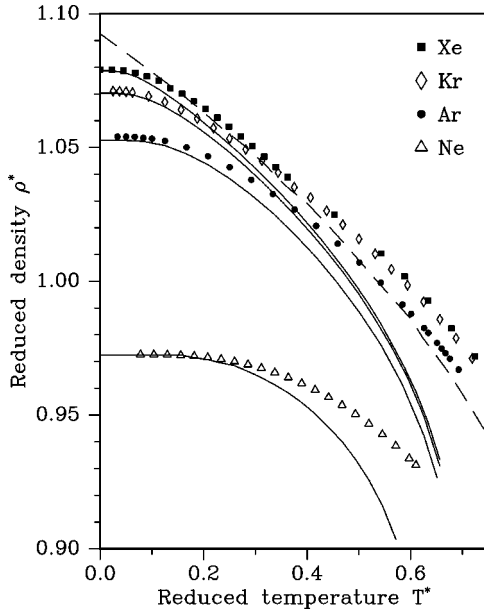


FIG. 3. Reduced density  $\rho^*$  vs reduced temperature  $T^* = T/\epsilon$  for the rare gases at atmospheric pressure. Experiments on Ne (Refs. 14 and 32), Ar (Refs. 32–34), Kr (Refs. 32 and 35), and Xe (Refs. 32,36 and 37): symbols as indicated in the figure. QHLD and MD results: solid and broken lines, respectively.

models that we have tried.<sup>6,13–17</sup> This discrepancy is one of the problems with the literature parameters mentioned in the Introduction.

The  $\rho^*$  versus  $h^*$  curve, which is found to deviate very little from a straight line, exhibits the expected trend towards a limiting density with increasing atomic number. The  $h^* = 0$  limit (infinite  $m$ ) is  $\rho^* = 1.092$ , the correct minimum-energy density for an fcc lattice of LJ particles.<sup>17</sup> For increasing  $h^*$  (decreasing  $m$ ), the zero-point effects become progressively more important and the lattice expands.

### C. Temperature dependence of the density

We report in Fig. 3 the densities as a function of  $T$ . The reduced experimental data for Xe, Kr, Ar, and Ne at atmospheric pressure are compared to the MD density (which in reduced units does not depend on the atomic species) and to the QHLD densities. With increasing  $T$ , quantum effects become less important and the experimental density difference among the various species decreases. The density differences, however, are still large when the melting temperature  $T_m^{\text{exp}}$  is reached. This observation indicates that, especially for neon, quantum effects are still significant even at melting.

Since it ignores all quantum effects, MD cannot distinguish between the different atomic species and overestimates the density at  $T=0$ , though only slightly for the heavier atoms. For very small  $T$ , MD predicts a thermal expansion linear in  $T$ , whereas experimentally the density is initially independent of  $T$ . This is a nonclassical zero-point effect, which is properly reproduced by the QHLD calculations. For large  $T$ , where the anharmonicity is large but quantum effects decrease, the MD results tend to agree with the experiments better than QHLD. As expected, the agreement is much better for Ar, Kr, and Xe than for Ne, which remains a quantum particle even close to the melting point.

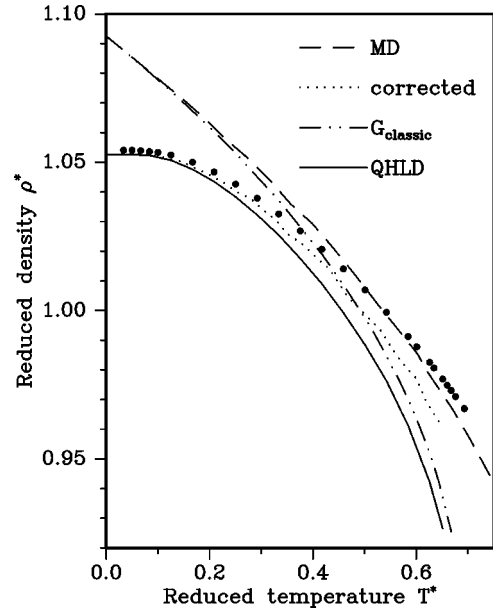


FIG. 4. Reduced density  $\rho^*$  vs reduced temperature  $T^*$  for Ar at atmospheric pressure. Experiments (Refs. 32–34): circles; MD calculations, “corrected” density, QHLD results with  $G$  and with  $G_{\text{classic}}$ : lines as indicated in the figure.

QHLD agrees with the experimental densities near to  $T = 0$  (for Ne, Kr, and Xe, by construction). As  $T$  is raised, QHLD predicts a thermal expansion larger than that experimentally observed, because of the neglect of the vibrational anharmonicity.<sup>8</sup> The discrepancy continues to increase, until we encounter a limiting temperature  $T_m$ , different for each atomic species, above which the QHLD calculations fails because no minimum of  $G$  can be found. The QHLD curves in Fig. 3 are truncated at  $T_m$ , which is found to be very close to the experimental melting temperature. Further discussion of this point is postponed to the next section.

The results shown in Fig. 3 confirm those of Fig. 1 and indicate that QHLD and MD are essentially complementary methods, since QHLD is accurate at low  $T$ , while MD is better at high  $T$ . We have found that QHLD calculations with  $G_{\text{classic}}$  provide a useful connection between the two methods, as shown for Ar in Fig. 4, where we compare the QHLD, MD, and  $G_{\text{classic}}$  densities,  $\rho_{\text{QHLD}}$ ,  $\rho_{\text{MD}}$ , and  $\rho_{\text{classic}}$ . At 0 K the  $\rho_{\text{classic}}$  and  $\rho_{\text{MD}}$  results coincide, since both structures correspond to the absolute minimum of the potential energy. As  $T$  is raised,  $\rho_{\text{classic}}$  progressively diverges from  $\rho_{\text{MD}}$ , because anharmonicity is increasing, and converges towards  $\rho_{\text{QHLD}}$ , as the quantum effects tend to decrease. The difference between  $\rho_{\text{MD}}$  and  $\rho_{\text{classic}}$  is solely due to anharmonicity, whereas the difference between  $\rho_{\text{QHLD}}$  and  $\rho_{\text{classic}}$  is only due to quantum effects. Therefore one can estimate the anharmonic corrections as  $\rho_{\text{MD}} - \rho_{\text{classic}}$ , and the quantum corrections as  $\rho_{\text{QHLD}} - \rho_{\text{classic}}$ . Since interactions between anharmonic and quantum effects are ignored, these are first-order estimates of the corrections.

By adding the anharmonic corrections to  $\rho_{\text{QHLD}}$ , or, equivalently the quantum corrections to  $\rho_{\text{MD}}$ , one gets a “corrected” density,  $\rho_{\text{corr}} = \rho_{\text{QHLD}} + \rho_{\text{MD}} - \rho_{\text{classic}}$  (also shown in Fig. 4). We find that the corrected densities agree with the experiments better than either  $\rho_{\text{QHLD}}$  or  $\rho_{\text{MD}}$ , with deviations around 0.7% on the average (2% in the worst

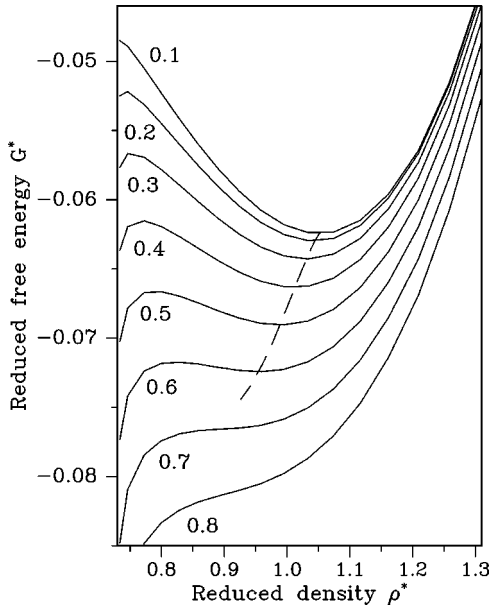


FIG. 5. The solid curves represent the reduced QHLD Gibbs free energy  $G^*(\rho^*=0, T^*)=G/\epsilon$  of Ar, computed as a function of the reduced density  $\rho^*$ , for several values of  $T^*$  (namely,  $T^*=0.1, 0.2, 0.3, \dots, 0.7, 0.8$ ), as indicated near each curve. The broken line represents the locus of the minima of  $G^*$ , as discussed in the text, followed from  $T^*=0$  to the disappearance of the minimum at  $T^*=0.651$ .

case) in the whole range of stability of solid Ne, Ar, Kr, and Xe. The anharmonic corrections are usually small, 1.6% on average and 3.5% in the worst case, and do not change very much with the atomic species. The quantum corrections are largest for Ne at 0 K (11%) and, as expected, decrease in the Ar, Kr, Xe sequence (3.4, 1.7, and 1.3%, respectively). By comparison, the deviations between experimental and calculated densities for van der Waals (i.e., molecular) crystals are usually found to be in the 1–5% range.<sup>2,8,9</sup> Our results confirm that this is indeed the typical accuracy of the MD and QHLD calculations themselves.

#### D. Thermal expansion mechanism and melting

Since the curvature of the interatomic potentials decreases with increasing distances, lattice expansion leads to smaller phonon frequencies and, consequently, to lower zero-point and entropic contributions to the free energy  $G$  [Eq. (1)]. The thermal expansion of the lattice is driven by the competition between the potential energy term  $\Phi_0$ , which favors structures close to mechanical equilibrium, and the entropic term, which favors expanded structures with smaller frequencies, and which becomes progressively more important as  $T$  increases. Figure 5 shows the Gibbs free energy  $G(p, T)$ , computed as a function of the density  $\rho$ , for argon at  $p=0$ , and for several values of  $T$ . At  $T \approx 0$ , where the only difference between  $\Phi_0$  and  $G$  is the zero-point energy, the equilibrium density is slightly lower than that yielding the minimum of  $\Phi_0$ . The equilibrium density decreases even further with increasing  $T$ , since the entropic effects increase. Eventually a critical temperature  $T_m$  is reached above which the minimum of  $G$  vanishes altogether: the QHLD model becomes unstable for  $T > T_m$ . To clarify this behavior we show in Fig. 5

the locus of the minima of  $G$ , which, by definition, represents  $G$  versus  $\rho$  along the curve of thermodynamic equilibrium. We have computed this curve as a parametric function of  $T$ ,  $G(0, T)$  versus  $\rho(0, T)$ , following  $T$  from 0 to the disappearance of the minimum, which for Ar occurs at  $T_m^*=0.651$  ( $T_m=78$  K).

The idea that melting is connected to an intrinsic instability of the solid goes back to Herzfeld and Goepfert Mayer<sup>24</sup> and has been discussed many times.<sup>25–30</sup> As convincingly argued by Ross and Wolf,<sup>30</sup> the various instability models consider the solid phase only, and therefore cannot describe genuine thermodynamic transitions between solid and liquid phases of equal Gibbs free energy. A correct prediction of the  $p, T$  melting curve requires an accurate calculation of the free energy in the two phases. However, the stability criteria<sup>25–27</sup> are still useful: loss of stability, although not necessarily exactly coincident with melting, cannot be too distant from it.<sup>9</sup>

A formal characterization of the instability  $T_m$  is obtained<sup>24–26</sup> by examining directly the conditions for the existence and stability of a local minimum of  $G$ :  $\partial G/\partial V=0$  and  $\partial^2 G/\partial V^2 > 0$ . Here we are considering stability with respect to small volume fluctuations away from the volume  $V(p, T)$  of thermodynamic equilibrium, i.e., we consider  $p$ ,  $T$ , and  $V$  as independently varying variables.<sup>31</sup> By expressing  $G$  in terms of the Helmholtz free energy  $F$ ,  $G(p, T)=pV+F(V, T)$ , the equilibrium and stability conditions reduce to  $p=-(\partial F/\partial V)_T$  (the state equations) and  $(\partial^2 F/\partial V^2)_T=\beta_T/V > 0$ , where  $\beta_T=-V(\partial p/\partial V)_T$  is the isothermal bulk modulus. It is the vanishing bulk modulus or, equivalently, the divergence of the isothermal compressibility  $k_T=1/\beta_T=-(\partial V/\partial p)_T/V$ , which is the origin of the instability at  $T_m$ .<sup>24–26</sup> This description is entirely consistent with what was observed in our QHLD computations.

In these computations, where  $G$  is numerically minimized by varying the molar volume  $V$  in a sequence of finite steps, we find that for  $T < T_m$  the volume converges to an equilibrium value, whereas for  $T > T_m$  the calculation fails because no minimum is found, as shown by Fig. 5. The QHLD instability temperatures  $T_m$  are compared in Table I with the experimental melting temperatures  $T_m^{\text{exp}}$  of the rare gases. In Fig. 3 the experimental points end near  $T_m^{\text{exp}}$ , whereas the QHLD curves are truncated at  $T_m$ . Notwithstanding the shortcomings due to the use of a solid-only melting criterion,<sup>30</sup> and to the neglect of the anharmonic contributions to the free energy,<sup>7</sup> the computed  $T_m$  follow quite closely the experimental data. As shown by Fig. 3, the QHLD calculations account for the quantum effects on melting, since they reproduce the observed decrease of the reduced  $T_m^{\text{exp}}$  for the lighter atoms. This is a purely quantum effect, as, according to the classical law of corresponding states, the reduced melting temperature of classical LJ particles should be independent of the atomic species.<sup>20</sup>

## V. CONCLUSIONS

We have computed the density of solid Ne, Ar, Xe, and Kr through QHLD, MD, and EM methods. In this way we have controlled the classical (MD), harmonic (QHLD), and static lattice (EM) approximations, i.e., estimated rather pre-

cisely their effects. Anharmonic effects are negligible at low temperatures and even close to the melting point they account only for a few percent of the density. Quantum effects are only important for very light atoms (Ne) and tend to decrease with increasing temperatures. Motional effects, which are usually large, decrease for large atomic masses, low temperatures, and high pressures.

We find that QHLD can be used to compute the structural parameters, with slowly degrading accuracy, for all temperatures up to that where the model becomes unstable. This breakdown temperature turns out to be a fair estimate of the melting point. The QHLD accuracy for the structural parameters is much better than that for the free energy. This result is not an artifact but a genuine property of the QHLD method, though we do not have yet a fully satisfactory explanation for it.

QHLD and MD are found to be complementary, rather than competing, methods. QHLD, where quantum effects are accounted for, but vibrational anharmonicity is neglected, is the better method at low temperatures. MD, which ignores all quantum effects but correctly handles large amplitude vibrations, is appropriate for solids close to the melting point and for fluids. The differences between MD and QHLD, in the range where both are valid, are small. Since QHLD is much more efficient than MD, we think that a QHLD computation should be one of the first steps in testing any proposed potential model, even for problems where disorder or large amplitude motion will eventually require MD or MC (Monte Carlo) techniques. If one wants to study the effects of pressure, rather than temperature, even a  $G_{\text{mech}}$  energy minimization (EM) can be a useful starting point. The EM

method, which neglects both quantum and anharmonic effects, is quite accurate for heavy molecules at low temperatures.

For a given problem it may be important to choose the fastest method among those applicable, as the speed differences are very large. For Ar on a fast RS/6000 work station we needed 0.2 sec for a EM calculation, 20 sec for a QHLD optimization, and 75 sec for a MD simulation with 256 atoms and 1000 timesteps, the minimum for barely acceptable equilibration and statistics. Though these times obviously depend on the specific problem, their ratios are expected to be quite typical.

It should be noticed that for Ne, Kr, and Xe we have fitted the potential models solely to the experimental density as a function of  $p$  at very low  $T$ . Though no  $T$  dependent data has been used in the fits, the models reproduce well the density as a function of  $T$ , within the accuracy of the calculation methods. These results provide some justification for the procedure of neglecting thermal effects while fitting a potential model. This approach, which is usually adopted because it is very convenient, is found to lead to acceptable results.

Our work shows that one can efficiently and accurately predict the structure of a solid phase, through the whole range of its thermodynamic stability, by using a suitable combination of EM, QHLD, and MD methods.

#### ACKNOWLEDGMENTS

Work done with funds from the University of Bologna ("Finanziamento speciale alle strutture"). We also thank MURST and CNR for further financial support.

- 
- <sup>1</sup>M. Born and K. Huang, *Dynamical Theory of Crystal Lattices* (Oxford University Press, New York, 1954).
- <sup>2</sup>A. J. Pertsin and A. I. Kitaigorodsky, *The Atom-Atom Potential Method* (Springer, Berlin, 1987).
- <sup>3</sup>W. Ludwig, *Recent Developments in Lattice Theory*, Springer Tracts in Modern Physics Vol. 43 (Springer-Verlag, Berlin, 1967).
- <sup>4</sup>V. N. Zharkov and V. A. Kalinin, *Equations of State for Solids at High Pressure and Temperature* (Consultants Bureau, New York, 1971).
- <sup>5</sup>T. H. K. Barron and M. L. Klein, in *Dynamical Properties of Solids*, edited by G. K. Horton and A. A. Maradudin (North-Holland, Amsterdam, 1974).
- <sup>6</sup>M. P. Allen and D. J. Tildesley, *Computer Simulation of Liquids* (Clarendon Press, Oxford, 1987).
- <sup>7</sup>D. J. Lacks and G. C. Rutledge, *J. Chem. Phys.* **101**, 9961 (1994).
- <sup>8</sup>R. G. Della Valle, E. Venuti, and A. Brillante, *Chem. Phys.* **198**, 78 (1995).
- <sup>9</sup>R. G. Della Valle, E. Venuti, and A. Brillante, *Chem. Phys.* **202**, 231 (1996).
- <sup>10</sup>R. G. Della Valle, E. Venuti, and A. Brillante, *Gazz. Chim. Ital.* **126**, 615 (1996).
- <sup>11</sup>L. Verlet, *Phys. Rev.* **159**, 98 (1967).
- <sup>12</sup>J. A. Barker, in *Rare Gas Solids*, edited by M. L. Klein and J. A. Venables (Academic Press, New York, 1977).
- <sup>13</sup>J. O. Hirschfelder, C. F. Curtiss, and R. B. Bird, *Molecular Theory of Liquid and Gases* (Wiley, New York, 1965).
- <sup>14</sup>D. N. Batchelder, D. L. Loose, and R. O. Simmons, *Phys. Rev.* **162**, 767 (1967).
- <sup>15</sup>R. K. Crawford, in *Rare Gas Solids*, edited by M. L. Klein and J. A. Venables (Academic Press, New York, 1977), p. 663.
- <sup>16</sup>K. Syassen and W. B. Holzapfel, *Phys. Rev. B* **18**, 5826 (1978).
- <sup>17</sup>C. Kittel, *Introduction to Solid State Physics* (Wiley, New York, 1996).
- <sup>18</sup>H. C. Andersen, *J. Chem. Phys.* **72**, 2384 (1980).
- <sup>19</sup>J. F. Fox and H. C. Andersen, *J. Phys. Chem.* **88**, 4019 (1984).
- <sup>20</sup>R. K. Pathria, *Statistical Mechanics* (Pergamon Press, Oxford, 1991).
- <sup>21</sup>M. S. Anderson and C. A. Swenson, *J. Phys. Chem. Solids* **36**, 145 (1975).
- <sup>22</sup>M. Grimsditch, P. Loubeyre, and A. Polian, *Phys. Rev. B* **33**, 7192 (1986).
- <sup>23</sup>M. S. Anderson, R. Q. Fugate, and C. A. Swenson, *J. Low Temp. Phys.* **10**, 345 (1973).
- <sup>24</sup>K. F. Herzfeld and M. Goeppert Mayer, *Phys. Rev.* **46**, 995 (1934).
- <sup>25</sup>L. L. Boyer, *Phys. Rev. Lett.* **42**, 584 (1979).
- <sup>26</sup>L. L. Boyer, *Phys. Rev. Lett.* **45**, 1858 (1980).
- <sup>27</sup>L. L. Boyer, *Phase Transit.* **5**, 1 (1985).
- <sup>28</sup>M. Born, *J. Chem. Phys.* **7**, 591 (1939).
- <sup>29</sup>J. L. Tallon, *Philos. Mag. A* **39**, 151 (1979).
- <sup>30</sup>M. Ross and G. Wolf, *Phys. Rev. Lett.* **57**, 214 (1986).
- <sup>31</sup>M. J. Sewell, *Maximum and Minimum Principles* (Cambridge University Press, Cambridge, 1987).

- <sup>32</sup>P. Korpiun and E. Lüscher, in *Rare Gas Solids*, edited by M. L. Klein and J. A. Venables (Academic Press, New York, 1977), p. 729.
- <sup>33</sup>O. G. Peterson, D. N. Batchelder, and R. O. Simmons, *Phys. Rev.* **150**, 703 (1966).
- <sup>34</sup>L. A. Schwalbe and R. W. Wilkins, *J. Chem. Phys.* **72**, 3130 (1980).
- <sup>35</sup>D. L. Loose and R. O. Simmons, *Phys. Rev.* **172**, 944 (1968).
- <sup>36</sup>D. R. Sears and H. P. Klug, *J. Chem. Phys.* **37**, 3002 (1962).
- <sup>37</sup>A. J. Eatwell and B. L. Smith, *Philos. Mag.* **6**, 461 (1961).